Nano Energy 88 (2021) 106221

Contents lists available at ScienceDirect

Nano Energy

journal homepage: www.elsevier.com/locate/nanoen

Cobalt single atom site isolated Pt nanoparticles for efficient ORR and HER in acid media

Lvhan Liang [a,b], Huihui Jin [a,c], Huang Zhou [a], Bingshuai Liu [a], Chenxi Hu [a], Ding Chen [a], Zhe Wang [c], Zhiyi Hu [a,d], Yufeng Zhao [e], Hai-Wen Li [f], Daping He [a,c,*], Shichun Mu [a,b,*]

[a] State Key Laboratory of Advanced Technology for Materials Synthesis and Processing, Wuhan University of Technology, Wuhan 430070, China
[b] Foshan Xianhu Laboratory of the Advanced Energy Science and Technology Guangdong Laboratory, Xianhu Hydrogen Valley, Foshan 528200, China
[c] Hubei Engineering Research Center of RF-Microwave Technology and Application, Wuhan University of Technology, Wuhan 430070, China
[d] NRC (Nanostructure Research Centre), Wuhan University of Technology, China
[e] Institute for Sustainable Energy/College of Sciences, Shanghai University, Shanghai 200444, China
[f] Platform of Inter/Transdisciplinary Energy Research, International Research Center for Hydrogen Energy, International Institute for Carbon-Neutral Energy Research, Kyushu University, Fukuoka 819-0395, Japan

ARTICLE INFO

Keywords:
Oxygen reduction reaction
Hydrogen evolution reaction
Metal-organic frameworks
Cobalt single atoms
Pt nanoparticles

ABSTRACT

Hitherto, developing an economical and stable high-activity bifunctional Pt catalyst for oxygen reduction reaction (ORR) and hydrogen evolution reaction (HER) becomes necessary for fuel cells and regeneration fuel cell system. However, how to uniformly disperse and firmly fix Pt nanoparticles (NPs) on carbon support with optimal particle size for catalysis is still a big challenge. Herein, by taking advantage of the isolating effect of the cobalt (Co) single atom site to Pt, strong interaction between Co single atoms and Pt, and the confinement of the porous carbon matrix derived metal organic frameworks, we successfully evenly immobilize Pt NPs on ZnCo-ZIF originated porous nitrogen-doped carbon matrix with rich cobalt single atoms (Co SAs-ZIF-NC) as multiple active sites. Compared with the commercial Pt/C catalyst, Pt@Co SAs-ZIF-NC, with ultralow Pt loading and ideal particle size, not only increases the active center, but also promotes the catalysis kinetics, greatly improving the ORR and HER catalytic activity. Under acidic conditions, its half-wave potential (0.917 V) is superior to commercial Pt/C (0.868 V), and the mass activity (0.48 A per mgPt) at 0.9 V is 3 times that of Pt/C (0.16 A per mgPt), surpassing the U.S. DOE target of 0.44 A per mgPt. Besides, it also shows outstanding HER performance. At 20 and 30 mV, its mass activity is even 4.5 and 13.6 times that of Pt/C. When further employed for HER in seawater, its mass activity is about 4 times as high as that of Pt/C, demonstrating the great potential applications.

1. Introduction

With the intensification of environmental pollution and traditional fossil fuel reserves facing crisis, sustainable and cost-efficient alternatives such as proton exchange membrane fuel cells (PEMFCs) is urgent [1]. The main factors limiting the development of PEMFCs include slow cathodic oxygen reduction kinetics and insufficient pure hydrogen product as anode fuel [2–4]. Therefore, it is imperative to find effective catalysts for oxygen reduction reaction (ORR) and hydrogen evolution reaction (HER) by electrochemical water splitting [5–9].

Hitherto, the most effective catalysts for ORR and HER are still platinum (Pt) based catalysts for fuel cells and regeneration fuel cells [10,11]. However, commercial Pt/C as the main catalyst for ORR and HER, does not have sufficient stability under severe conditions, heavily limiting its large-scale use [12–16]. For promoting the industrialization of PEMFCs, reducing the dosage of Pt and enhancing the stability of Pt-based catalysts is the top priority [17–20]. For a long time, to reduce the amount of Pt, researches have been devoted to preparing highly efficient Pt catalysts [21], including alloying with non-precious metals or reducing the size of platinum particles [22–26]. However, the preparation conditions of the alloy are harsh, and the size of Pt particles is difficult to control [27,28]. As reported, selecting suitable support to adjust the size of Pt particles with enhanced active sites is a facile and effective method to prepare highly active Pt-based catalysts [29].

* Corresponding authors at: State Key Laboratory of Advanced Technology for Materials Synthesis and Processing, Wuhan University of Technology, Wuhan 430070, China.
E-mail addresses: hedaping@whut.edu.cn (D. He), msc@whut.edu.cn (S. Mu).

https://doi.org/10.1016/j.nanoen.2021.106221
Received 20 January 2021; Received in revised form 8 May 2021; Accepted 1 June 2021
Available online 7 June 2021

In recent years, since large specific surface area, coordinated aperture size and abundant nitrogen content, zeolite-based imidazole frameworks (ZIFs) have been confirmed suitable for preparing precursors of tailor-made carbon-based materials, [30–36]. Furthermore, ZIF-derived carbon materials doped with transition metals (Fe, Co, Ni, Cu, etc.) have shown excellent ORR or HER activity [37]. Thus, their high intrinsic activity and large specific surface area make them outstanding supports for noble metal for efficient electrocatalysis [38, 39]. For example, Chong et al. chose Co-based or bimetallic Zn-Co zeolite imidazole framework to produce Co sites by pyrolysis, then impregnated the Pt source, and obtained the PtCo alloy through further thermally activation. Compared with commercial Pt/C, it has higher activity and stability in fuel cells [40]. Yin et al. synthesized single Co atom with precise N coordination, making it useful as a high-quality oxygen reduction catalyst under alkaline conditions [3].

Inspired by the synergetic catalytic effect of Co sites in MOF-originated materials, to prepare a high-efficiency bifunctional low-Pt catalyst, here Co single atom sites in porous N-doped carbon are proposed to isolate and anchor Pt NPs, limiting the growth of Pt NPs. Thus, carbon-based materials with Co single atoms (Co SAs-ZIF-NC) derived from bimetallic ZIFs (ZnCo-ZIF) can be chosen as support for Pt NPs. Benefiting from the porous structure and the isolating-anchoring effect of cobalt atom sites, Pt NPs, with ideal particle size, are immobilized on N-doped carbon materials (Pt@Co SAs-ZIF-NC). In terms of the synergistic effect of Pt NPs and Co ZIF-NC catalysis system, Pt@Co SAs-ZIF-NC shows excellent ORR and HER performance under acidic and seawater conditions.

2. Results and discussion

2.1. Synthesis and structural characterization

As depicted in Scheme 1, ZnCo-ZIF was first synthesized, subsequently heated to 900 °C under nitrogen atmosphere, and naturally cooled to obtain cobalt single atoms that confined in N-doped carbon matrix (Co SAs-ZIF-NC). After that, Co SAs-ZIF-NC was reacted with H_2PtCl_6 solutions at 70 °C to get H_2PtCl_6@Co SAs-ZIF-NC. Finally, H_2PtCl_6@Co SAs-ZIF-NC was reduced at 300 °C for 1 h under 5% H_2/Ar atmosphere to obtain Pt NPs anchored by single cobalt atoms (Pt@Co SAs-ZIF-NC). The same experiment was performed on ZIF-67 and ZIF-8, and Pt loaded N-doped carbon matrix with cobalt NPs (Pt@Co ZIF-NC) and Pt loaded N-doped carbon matrix (Pt@ZIF-NC) were obtained, respectively.

From scanning electron microscope (SEM) (EIS, Fig. S1a, b), and transmission electron microscope (TEM) images (EIS, Fig. S1c, d), the as-synthesized Co SAs-ZIF-NC is uniform in size and presents a regular dodecahedron. As seen from Fig. S1e, f and S1g, h, Pt NPs are scattered on the appearance of Co SAs-ZIF-NC uniformly. The high-resolution TEM (HRTEM) image (Figs. 1**a**, S2) shows that the main size of Pt particles in Pt@Co SAs-ZIF-NC is concentrated in 2–4 nm (about 3.32 nm in average). Fig. 1**d** displays that Pt NPs in Pt@Co SAs-ZIF-NC are fixed in the carbon matrix, and the lattice fringes with a pitch of 0.23 nm correspond to the (111) plane of metallic Pt NPs. While high angle annular dark field scanning TEM (HAADF-STEM) demonstrates that Co predominantly exists in the form of single atoms located around Pt NPs (Figs. 1**e**, S3). In contrast, although Pt@ZIF-NC also shows a regular rhombohedral dodecahedron (Figs. 1**b**, S4), its Pt NPs are uneven and randomly distributed. At the same time, for Pt@Co ZIF-NC, its structure is damaged and becomes irregular due to the massive agglomeration of Co particles, and Pt particles are too large and arrange randomly (Figs. 1**c**, S5). These will greatly affect the activity and efficiency of Pt catalysts. HAADF-STEM images and homologous EDX element mappings (Fig. 1**f–j**) further demonstrate uniform distribution of Co and nano-aggregated Pt. The Pt loading in Pt@Co SAs-ZIF-NC is 5.01 wt% detected with ICP-OES (Table S1).

From the X-ray diffraction (XRD) pattern (Fig. 2**a**), Pt@Co SAs-ZIF-NC and Co SAs-ZIF-NC possess a broad peak at approximately 25°, which is attributed to the C (002) plane. The diffraction peaks located at $2\theta = 39.9°$, 46.4°, and 67.8° belong to (111), (200), and (220) planes of Pt, respectively, indicating the crystal structure of Pt NPs in Pt@Co SAs-ZIF-NC is face-centered cubic (fcc).

Due to the spin orbit interaction, the high-resolution Pt 4f spectrum of X-ray photoelectron spectroscopy (XPS) can be fitted to Pt $4f_{7/2}$ (71.3 eV and 74.65 eV) and Pt $4f_{5/2}$ (72.6 eV and 75.58 eV) (Fig. 2**b**), matching with Pt^0 and Pt ions (Pt^{2+} and Pt^{4+}), separately [41–43]. Compared with Pt/C, a negative shift (0.25 eV) of binding energy is adverted for the Pt 4f doublet on Pt@Co SAs-ZIF-NC, while the shift of Pt@Co ZIF-NC is 0.15 eV (EIS, Fig. S6). The binding energies of Co $2p_{3/2}$ peaks for Pt@Co SAs-ZIF-NC and Pt@Co ZIF-NC are 780.7 eV, 782.9 eV, 786.3 eV and 779.4 eV, 782.2 eV, 786.3 eV, respectively (Fig. 2**c, d**). Compared with Co^0 (778.1–778.8 eV), Co^{2+} (780.9 eV) and Co^{3+} (779.8 eV) [29,44,45], there is more nature of ion $Co^{\delta+}$ ($0 < \delta < 3$) of Co in Pt@Co SAs-ZIF-NC, while Pt@Co ZIF-NC possesses more Co^0 (NPs). By comparison with Co SAs-ZIF-NC (781.0 eV, 783.2 eV, 786.6 eV) (EIS, Fig. S7a, b), after anchoring Pt NPs, the binding energy of Co $2p_{3/2}$ peaks in Pt@Co SAs-ZIF-NC exhibits a negative shift. From the XPS spectrum of N 1s, the content of graphitic N in Pt@Co SAs-ZIF-NC increases significantly in comparison with that of Co SAs-ZIF-NC. With the increased graphitic N, it could attract more electrons from the neighboring C atoms and provide more electrons to Co and Pt, which leads to the negative shift of Pt and Co [46,47]. All N 1s XPS spectra in Co SAs-ZIF-NC, Pt@Co SAs-ZIF-NC and Pt@Co ZIF-NC have three dividing peaks, representing pyridinic N (398.8 eV), pyrrolic N (400 eV), and graphitic N (401.2 eV) [44]. Among them, Pt@Co SAs-ZIF-NC and Co SAs-ZIF-NC possess an enhanced pyridinic N and graphitic N (Figs. 2**e, f** and S7). The increased pyridinic N in can greatly reduce the localization of electrons around the cobalt center, improve the interaction with oxygen-containing species, and reduce the energy barrier of the intermediate [48]. Besides, the graphitic N bonded with three carbon atoms leaves a lone electron, which can be contributed to a Pt atom to transform its electron layout.

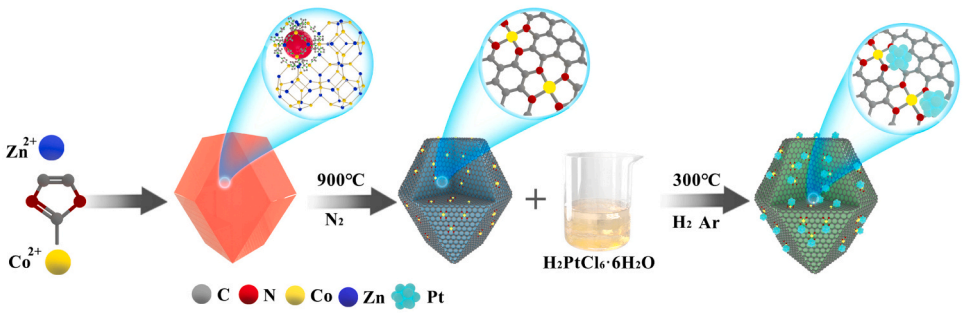

Scheme 1. Schematic diagram of the synthesis for Pt@Co SAs-ZIF-NC.

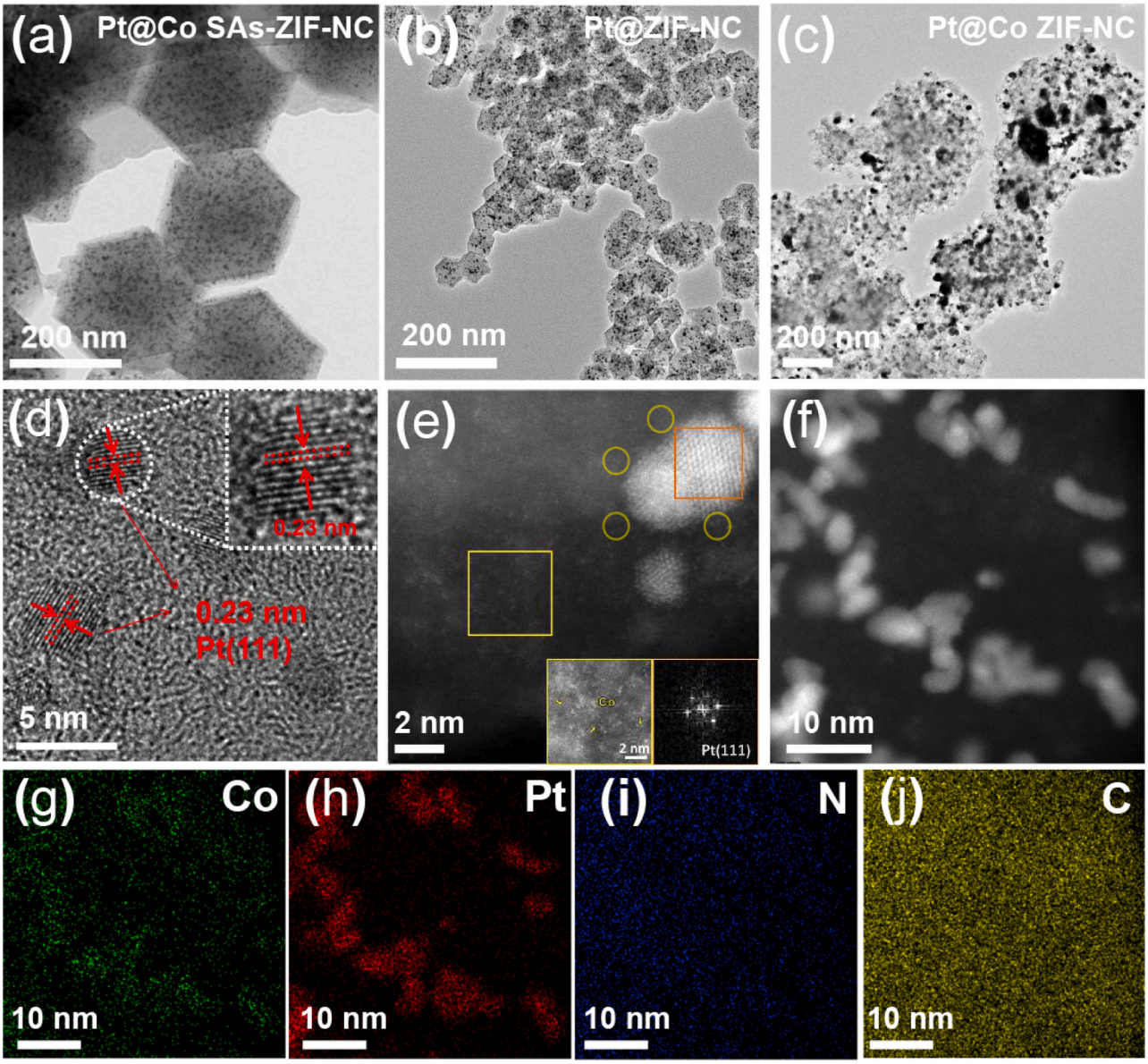

Fig. 1. HRTEM image of (a) Pt@Co SAs-ZIF-NC, (b) Pt@ZIF-NC, (c) Pt@Co ZIF-NC. (d) Magnifying HRTEM image of Pt@Co SAs-ZIF-NC. (e) HAADF-STEM image of Pt@Co SAs-ZIF-NC, corresponding FFT of the area indicated by the orange box, enlarged area indicated by the yellow box, the yellow circle encircles the cobalt single atom. (f–j) EDX elemental maps of Pt@Co SAs-ZIF-NC: Co (green), Pt (red), N (blue) and C (yellow).

2.2. Oxygen reduction catalysis

Firstly, the ORR catalytic activity of catalysts with different loadings was explored. As shown in Fig. S8, when the load capacity reaches to 20 μL (25 ugPt cm^{-2}), the catalyst has the best half-wave potential ($E_{1/2}$) and mass activity. Then, based on the Pt loading, a more in-depth electrocatalytic investigation was carried out. Fig. 3**a** exhibits the cyclic voltammetry (CV) curves of all catalysts amid 0 and 1.2 V (vs RHE) in N_2-saturated 0.1 M $HClO_4$. The adsorption and desorption peaks of hydrogen can be observed in the region of $0 < E < 0.4$ V, and the electrochemical surface area (ECSA) of Pt@Co SAs-ZIF-NC (71 m^2 per g Pt) is on a par with Pt/C (70 m^2 per g Pt), while which of Pt@Co ZIF-NC (52 m^2 per g Pt) and Pt@ZIF-NC (58 m^2 per g Pt) is lower.

Fig. 3**b** presents the linear sweep voltammetry (LSV) curves of the five catalysts. Their ORR catalytic capability is in order: Pt@Co SAs-ZIF-NC > Pt/C > Pt@Co ZIF-NC > Pt@ZIF-NC > Co SAs-ZIF-NC. Compared with Pt/C ($E_{1/2}$ = 0.868 V, onset potential =0.94 V), the half-wave potential (0.919 V) and onset potential (1.05 V) of Pt@Co SAs-ZIF-NC are significantly improved, which rivals most reported noble metal catalysts (Table S2). The Tafel slope of Pt@Co SAs-ZIF-NC is 62 mV dec^{-1}, lower than that of Pt/C (78 mV dec^{-1}), Pt@Co ZIF-NC (95 mV dec^{-1}), Pt@ZIF-NC (94 mV dec^{-1}) and Co SAs-ZIF-NC (64 mV dec^{-1}), suggesting that Pt@Co SAs-ZIF-NC has a faster ORR kinetics than Pt/C and the other three catalysts (Fig. 3**c**). To further explore the reaction mechanism of Pt@Co SAs-ZIF-NC, LSV testing under different speeds of 625–2500 rpm were performed. As the speed increases, the onset potential remains constant and the current density gradually increases (EIS, Fig. S9a). Koutecky-Levich (K-L) diagram of Pt@Co SAs-ZIF-NC shows a very good linear relationship at different potentials (EIS, Fig. S9b), indicating the electron transfer number of each oxygen molecule in the ORR is basically the same. And the average electron transfer number of Pt@Co SAs-ZIF-NC is 3.9, demonstrating that its ORR process is highly close to four-electron transfer.

Furthermore, the mass activity of Pt@Co SAs-ZIF-NC was calculated to be 2.8 A/mgPt at 0.85 V (vs RHE), 6 times that of commercial Pt/C catalyst (0.45 A/mgPt) (Fig. 3**d**). When the potential reaches 0.9 V (vs

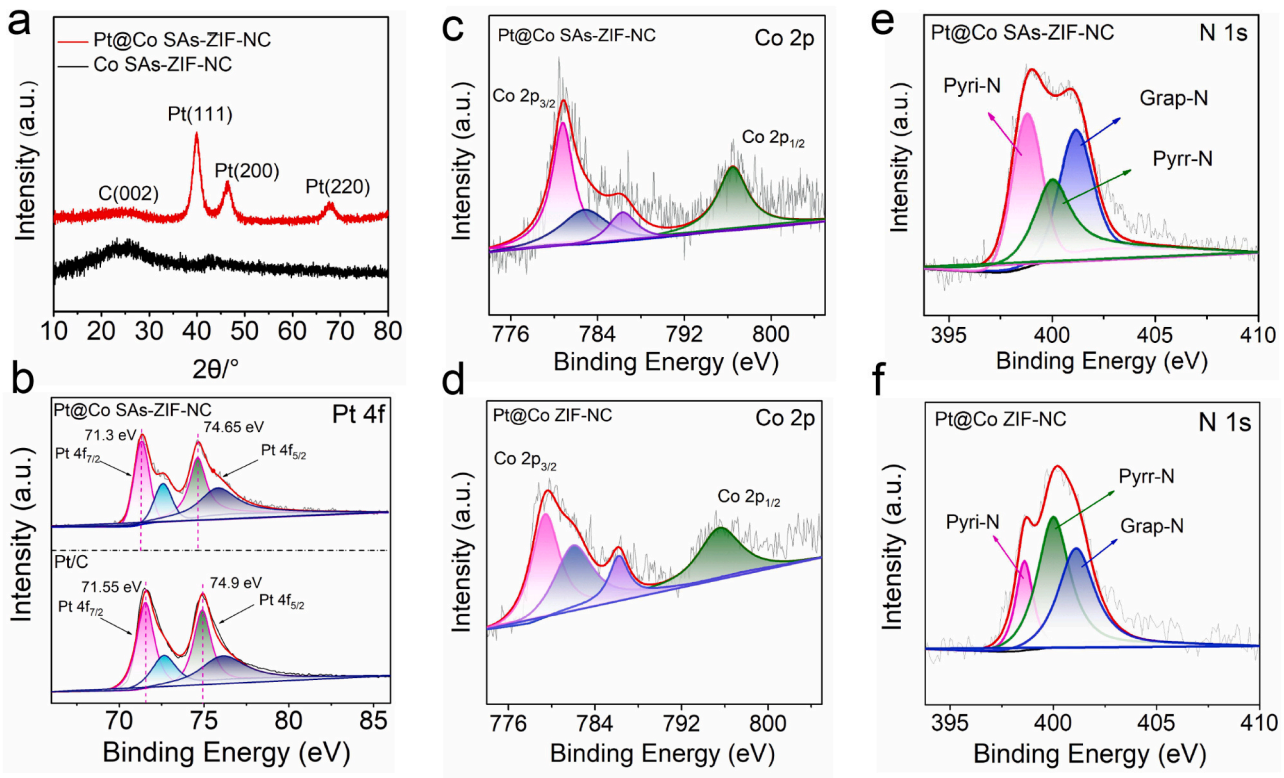

Fig. 2. (a) XRD pattern. (b) XPS spectrum of Pt 4f for Pt@Co SAs-ZIF-NC and Pt/C. (c) Co 2p spectrum for Pt@Co SAs-ZIF-NC. (d) Co 2p spectrum for Pt@Co ZIF-NC. (e) N 1s spectrum for Pt@Co SAs-ZIF-NC. (f) N 1s for Pt@Co ZIF-NC.

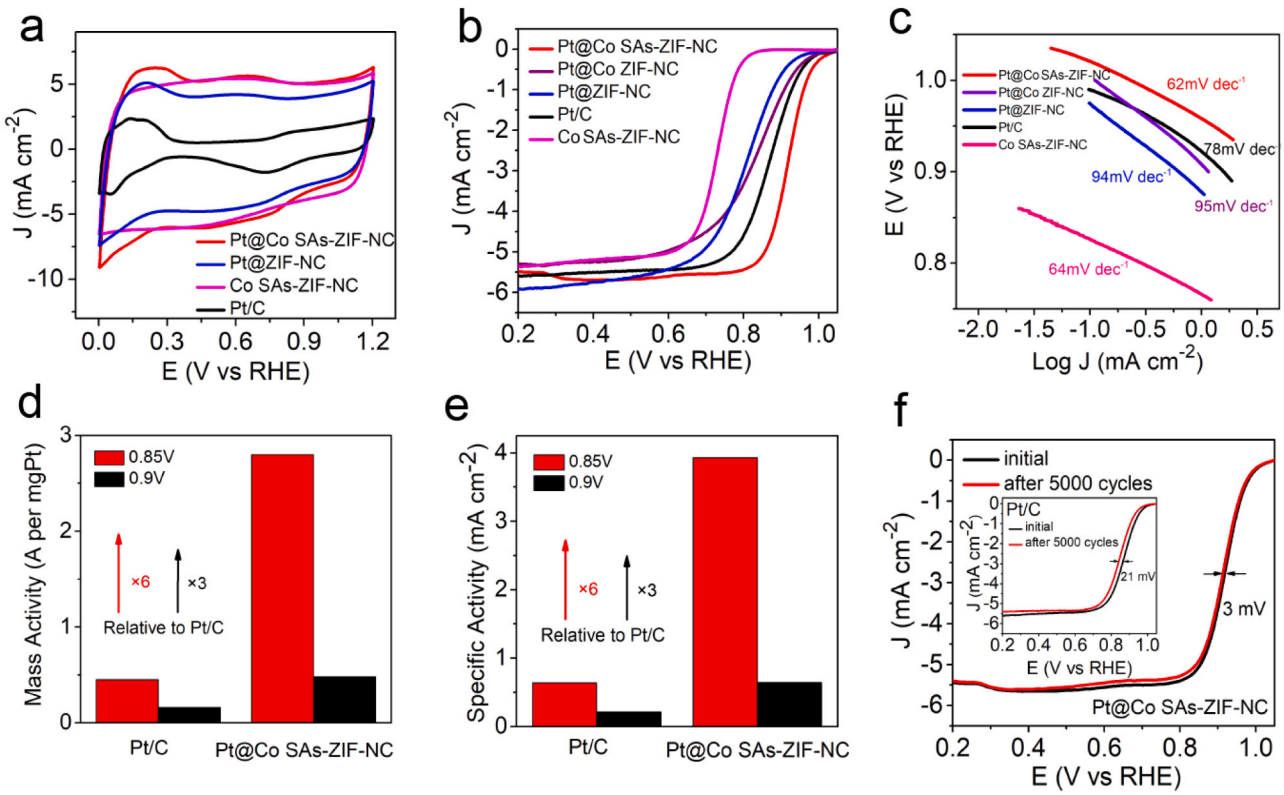

Fig. 3. (a) CV curves recorded in N_2 saturated 0.1 M $HClO_4$ solution. (b) ORR polarization curves and (c) Tafel slopes of Pt@Co SAs-ZIF-NC, Pt@Co ZIF-NC, Pt@ZIF-NC, Pt/C and Co SAs-ZIF-NC. (d) Mass activity and (e) specific activity of Pt@Co SAs-ZIF-NC and Pt/C at 0.85 and 0.9 V for ORR. (f) ORR polarization curves of Pt@Co SAs-ZIF-NC and commercial Pt/C (inset) before and after 5000 cycles.

RHE), its mass activity (0.48 A/mgPt) is still 3 times that of Pt/C (0.16 A/mgPt) and surpass the 2020 U.S. Department of Energy target (0.44 A/mgPt). In addition, as shown in Fig. 3**e**, the specific activity of Pt@Co SAs-ZIF-NC at 0.85 V (vs RHE) and 0.9 V are 3.9 mA cm^2 and 0.64 mA cm^2, which are 6 times and 3 times higher than that of Pt/C (0.64 mA cm^2 at 0.85 V, 0.21 mA cm^2 at 0.9 V), respectively.

The stability test was then measured with accelerating cycling between 0.65 and 1.0 V in O_2 saturated 0.1 M $HClO_4$ solution. After 5000 cycles, the half-wave potential of Pt@Co SAs-ZIF-NC is only 3 mV less than before, whereas it is 21 mV of Pt/C (Fig. 3**f**). And the morphology of Pt@Co SAs-ZIF-NC is basically stable after the CV acceleration (EIS, Fig. S10a, b), whose particle size only changes from the original 3.32–3.42 nm (EIS, Fig. S10c, d). The stability tests were measured by current versus time (i-t) chronoamperometric response at applied bias voltage of 0.69 V for 40,000 s. As shown in Fig. S11, the normalized current loss of Pt@Co SAs-ZIF-NC is only 11.9%, much smaller than commercial Pt/C (29.12%).

2.3. Hydrogen evolution catalysis

HER properties were first detected at ambient temperature in 0.5 M H_2SO_4 electrolytes. According to Fig. 4**a**, Pt@Co SAs-ZIF-NC shows splendid HER catalytic activity, where the initial overpotential is only 15 mV, and it requires merely 27 mV overpotential when the current density is 10 mA cm^{-2}, preceding Pt/C (34 mV), Pt@Co ZIF-NC (37 mV), Pt@ZIF-NC (37 mV) and the most reported Pt-based catalysts (Figs. 4**b**, S13, Table S3). In addition, it is far better than that of Co SAs-ZIF-NC (261 mV@10 mA cm^{-2}) (EIS, Fig. S14). Similarly, when the current density reaches 50 mA cm^{-2}, it barely needs 34 mV overpotential, while Pt/C, Pt@Co ZIF-NC and Pt@ZIF-NC require 45 mV, 48 mV and 55 mV overpotential, respectively. As exhibited in Fig. 4**c**, Tafel slope values of Pt@Co SAs-ZIF-NC, Pt@Co ZIF-NC, Pt@ZIF-NC and Pt/C are 21, 19, 28 and 21 mV dec^{-1}, respectively. According to the classical theory, the Tafel mechanism should be mainly responsible for their HER processes [39,49,50]. Notably, the Nyquist diagram shows that Pt@Co SAs-ZIF-NC has lower charge transfer resistance when compared with Pt@Co ZIF-NC and Pt@ZIF-NC, and also slightly smaller than Pt/C (Fig. 4**d**), indicating that the mass diffusion process and the

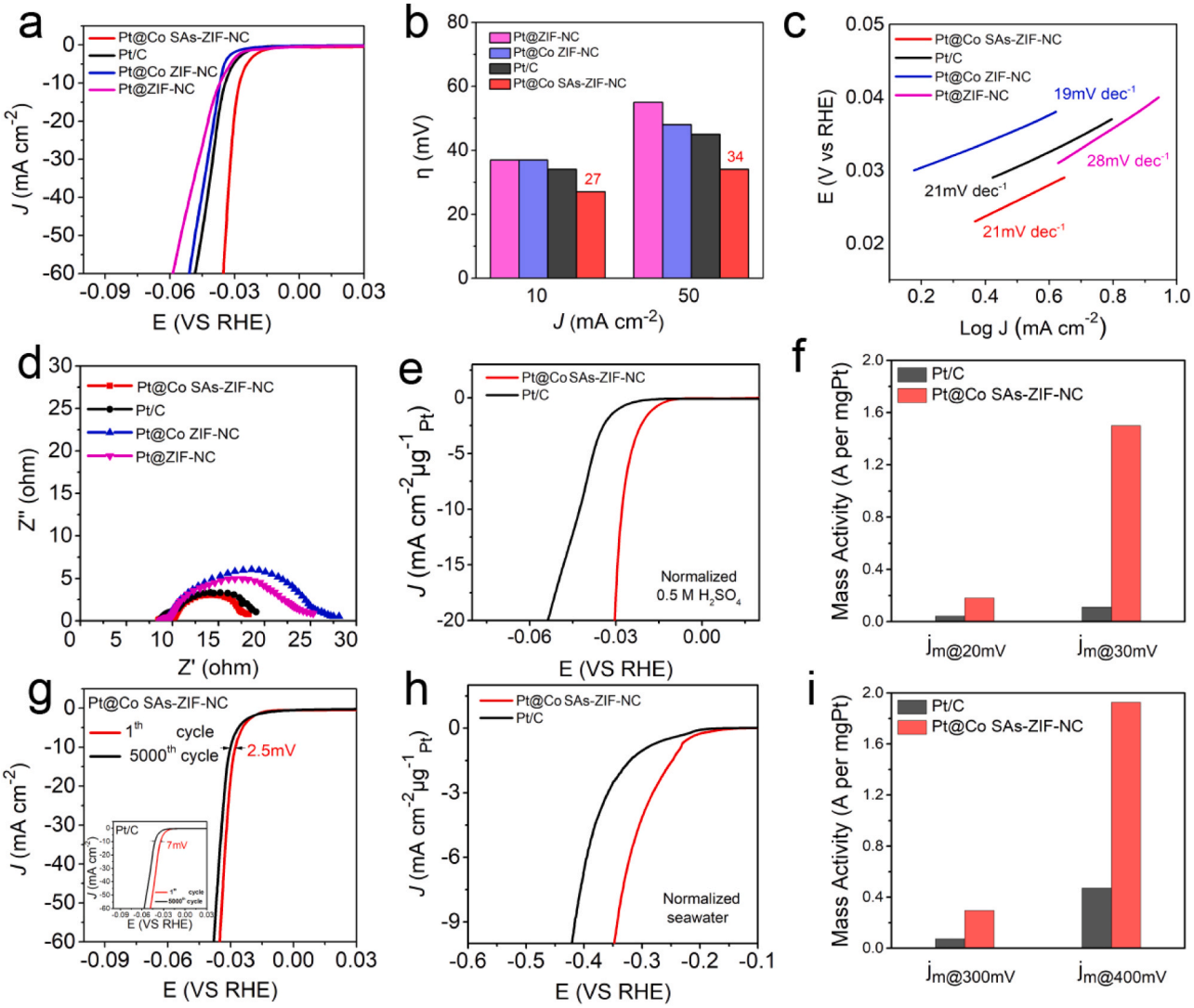

Fig. 4. (a) HER polarization curves of Pt@Co SAs-ZIF-NC, Pt@Co ZIF-NC, Pt@ZIF-NC and Pt/C in 0.5 M H_2SO_4 electrolyte at a scan rate of 5 mV s^{-1}. (b) Corresponding overpotentials (j = 10/50 mA cm^{-2}). (c) Tafel plots. (d) Electrochemical impedance spectroscopy (EIS) collected in the frequency range of 0.01–10^5 Hz. (e) LSV curves normalized by loaded Pt on electrodes. (f) Mass activity of Pt@Co SAs-ZIF-NC and Pt/C at 20 and 30 mV. (g) Polarization curves of Pt@Co SAs-ZIF-NC and Pt/C (inset) before and after 5000 CV cycles. (h) LSV curves in the seawater normalized by Pt loading on electrodes. (i) Mass activity of Pt@Co SAs-ZIF-NC and Pt/C at 300 and 400 mV in the seawater.

charge transfer are accelerated at the Pt@Co SAs-ZIF-NC electro-de-electrolyte interface.

To further explore the intrinsic activity, LSV curves for Pt@Co SAs-ZIF-NC and Pt/C was normalized by Pt loading (Fig. 4**e**), then their mass activity was calculated. As shown in Fig. 4**f**, at 20 and 30 mV, the mass activity of Pt@Co SAs-ZIF-NC is 0.18 and 1.5 A/mgPt, respectively, which is 4.5 and 13.6 times as much as that of Pt/C. In terms of stability testing, Pt@Co SAs-ZIF-NC is almost overlapped with the original LSV curve (only increase of 2.5 mV) after 5000 cycles, while Pt/C increases by 7 mV after 5000 cycles (Fig. 4**g**). In addition, it can be seen that the morphology of Pt@Co SAs-ZIF-NC is basically stable after the CV acceleration (EIS, Fig. S15a, b), and there is no binding energy shift of Pt 4f and Co 2p peaks for Pt@Co SAs-ZIF-NC through XPS analysis (EIS, Fig. S16a, b). The above results manifest that Pt@Co SAs-ZIF-NC owns better activity and stability in acidic media.

Moreover, Pt@Co SAs-ZIF-NC was employed for hydrogen evolution in seawater, and its catalytic performance is basically the same as that of Pt/C (EIS, Fig. S17). But when the LSV (Fig. 4**h**) was normalized by Pt loading, it can be calculated that, at 300 and 400 mV, its mass activity of Pt@Co SAs-ZIF-NC (0.29 and 1.93 A/mgPt) is about 4 times that of Pt/C (0.072 and 0.47 A/mgPt) (Fig. 4**i**), showing its potential usability.

2.4. Discussion

For the limit of Co active sites to Pt NPs, first of all, from the HRTEM of Pt@Co SAs-ZIF-NC, Pt@Co ZIF-NC, Pt@ZIF-NC, it can be clearly seen that the Pt NPs in Pt@Co SAs-ZIF-NC have a more uniform and ideal size and a more suitable particle distribution. Compared with Pt@ZIF-NC, the Co sites of Pt@Co SAs-ZIF-NC do play a role in isolating Pt NPs. In addition, compared with the Co NPs in Pt@Co ZIF-NC, the Co in Pt@Co SAs-ZIF-NC exists more in the form of single atoms, indicating that the single Co atom in uniform distribution can anchor Pt. Furthermore, relatively to commercial Pt/C, the negative shift of the binding energy is 0.25 eV for the Pt 4f peak in Pt@Co SAs-ZIF-NC, while for Pt@Co ZIF-NC, with the presence of Co metallic particles, its shift is only 0.15 eV. This further proves the stronger interaction between Co single atoms and Pt NPs in Pt@Co SAs-ZIF-NC, due to the effect of Co single atoms on Pt NPs, which promotes the anchoring of Co to Pt. Also, the confinement of porous carbon can contribute to limiting the Pt growth. As a result, Pt NPs are homogenously restricted to a specific area and maintain a relatively uniform particle size, which improves the utilization of Pt.

The excellent ORR and HER electrocatalytic activity and stability of Pt@Co SAs-ZIF-NC can be explained as follows: 1) More suitable particle size distribution and even dispersion of Pt NPs are beneficial to enhancing the electrocatalytic performance; 2) Co SAs-ZIF-NC as the support also provides a large number of active sites (such as Co-N_x) for the catalyst, besides, the enhanced content of pyridinic N and graphitic N also has a positive effect on electron transfer and catalytic activity; 3) The synergy between Pt NPs and Co SAs-ZIF-NC in Pt@Co SAs-ZIF-NC further promotes the electrocatalytic performance. Especially for ORR, compared with Pt/C and Co SAs-ZIF-NC, Pt@Co SAs-ZIF-NC has higher half-wave potential, ECSA, mass activity and stability, and is also better than other Pt-based catalysts such as Pt@ZIF-NC. Therefore, the synergistic effect is fully demonstrated.

3. Conclusion

In summary, by isolating Pt nanoparticles on porous nitrogen-doped carbon in terms of Co single atom sites (Co SAs-ZIF-NC), strong interaction between Co single atoms and Pt, and confined growth of Pt nanoparticles in porous carbon matrix, we successfully obtained the well dispersed Pt nanocatalysts with ideal particle size. The prepared Pt@Co SAs-ZIF-NC with more active center types and sites for electrocatalysis, significantly increasing the use efficiency of Pt catalysts. As a result, whether for ORR and HER, it always possesses superior activity and stability than commercial platinum carbon. Its ORR mass activity at 0.9 V in acidic media is 3 times that of commercial Pt/C catalysts, beyond the U.S. DOE target and most of the literature reports of Pt catalysts. In addition, its HER mass activity in acidic media and seawater is also a multiple of Pt/C. Therefore, our work provides a promising method for designing and constructing highly active and stable next-generation Pt-based catalysts with multiple active centers, which significantly reduces the dosage of Pt. The results show that our Pt@Co SAs-ZIF-NC catalyst has great application prospects in fuel cells and other applications.

CRediT authorship contribution statement

Shichun Mu, Daping He: Conceptualization, Writing - review & editing, Validation. **Lvhan Liang**: Methodology, Writing - original draft preparation. **Huihui Jin, Huang Zhou**: Software. **Bingshuai Liu, Chenxi Hu, Zhiyi Hu**: Data curation. **Zhe Wang, Yufeng Zhao**: Visualization. **Ding Chen, Hai-Wen Li**: Investigation.

Declaration of Competing Interest

The authors declare that they have no known competing financial interests or personal relationships that could have appeared to influence the work reported in this paper.

Acknowledgments

This work was supported by the National Natural Science Foundation of China (22075223, 51701146), and the State Key Laboratory of Advanced Technology for Materials Synthesis and Processing (Wuhan University of Technology) (2021-ZD-4).

Appendix A. Supporting information

Supplementary data associated with this article can be found in the online version at doi:10.1016/j.nanoen.2021.106221.

References

[1] R. Borup, J. Meyers, B. Pivovar, Y.S. Kim, R. Mukundan, N. Garland, D. Myers, M. Wilson, F. Garzon, D. Wood, P. Zelenay, K. More, K. Stroh, T. Zawodzinski, X. J. Boncella, J.E. Mcgrath, O.M. Inaba, K. Miyatake, M. Hori, K. Ota, Z. Ogumi, S. Miyata, A. Nishikata, Z. Siroma, Y. Uchimoto, K. Yasuda, K. Kimijima, N. Iwashita, Scientific aspects of polymer electrolyte fuel cell durability and degradation, Chem. Rev. 107 (2007) 3904–3951.

[2] Y. Chen, S. Ji, Y. Wang, J. Dong, W. Chen, Z. Li, R. Shen, L. Zheng, Z. Zhuang, D. Wang, Y. Li, Isolated single iron atoms anchored on N-doped porous carbon as an efficient electrocatalyst for the oxygen reduction reaction, Angew. Chem. 129 (2017) 7041–7045.

[3] P. Yin, T. Yao, Y. Wu, L. Zheng, Y. Lin, W. Liu, H. Ju, J. Zhu, X. Hong, Z. Deng, G. Zhou, S. Wei, Y. Li, Single cobalt atoms with precise N-coordination as superior oxygen reduction reaction catalysts, Angew. Chem. Int. Ed. 55 (2016) 10800–10805.

[4] X. Huang, Z. Zhao, L. Cao, Y. Chen, E. Zhu, Z. Lin, M. Li, A. Yan, A. Zettl, Y. M. Wang, X. Duan, T. Mueller, Y. Huang, High-performance transition metal-doped Pt_3Ni octahedra for oxygen reduction reaction, Science 348 (2015) 1230–1234.

[5] L. Jiao, R. Zhang, G. Wan, W. Yang, X. Wan, H. Zhou, J. Shui, S. Yu, H. Jiang, Nanocasting SiO_2 into metal-organic frameworks imparts dual protection to high-loading Fe single-atom electrocatalysts, Nat. Commun. 11 (2020) 2831.

[6] Y. Zhao, T. Ling, S. Chen, B. Jin, A. Vasileff, Y. jiao, L. Song, J. Luo, S. Qiao, Non-metal single Iodine atom electrocatalysts for the hydrogen evolution reaction, Angew. Chem. Int. Ed. 58 (2019) 12252–12257.

[7] H. Zhou, T. Yang, Z. Kou, L. Shen, Y. Zhao, Z. Wang, X. Wang, Z. Yang, J. Du, J. Xu, M. Chen, L. Tian, W. Guo, Q. Wang, H. Lv, W. Chen, X. Hong, J. Luo, D. He, Y. Wu, Negative Pressure Pyrolysis Induced Highly Accessible single sites dispersed on 3D graphene frameworks for enhanced oxygen reduction, Angew. Chem. Int. Ed. 59 (2020) 20465–20469.

[8] T. Wang, C. Yang, Y. Liu, M. Yang, X. Li, Y. He, H. Li, H. Chen, Z. Lin, Dual-shelled multidoped hollow carbon nanocages with hierarchical porosity for high-performance oxygen reduction reaction in both alkaline and acidic media, Nano Lett. 20 (2020) 5639–5645.

[9] C. Wei, Y. Sun, G.G. Scherer, A.C. Fisher, M. Sherburne, J.W. Ager, Z.J. Xu, Surface composition dependent ligand effect in tuning the activity of nickel-copper bimetallic electrocatalysts toward hydrogen evolution in alkaline, J. Am. Chem. Soc. 142 (2020) 7765–7775.

[10] W. Li, Y. Xiong, Z. Wang, M. Bao, J. Liu, D. He, S. Mu, Environmental seed-mediated synthesis of large-diameter ternary TePtCo nanotubes for enhanced oxygen reduction reaction, Appl. Catal. B Environ. 231 (2018) 277–282.
[11] Z. Song, Y. Zhu, H. Liu, M.N. Banis, L. Zhang, J. Li, K. Doyle-davis, R. Li, T. Sham, L. Yang, A. Young, G.A. Botton, L. Liu, X. Sun, Engineering the Low coordinated Pt single atom to achieve the superior electrocatalytic performance toward oxygen reduction, Small 16 (2020), 2003096.
[12] H. Jin, H. Zhou, D. He, Z. Wang, Q. Wu, Q. Liang, S. Liu, S. Mu, Environmental MOF-derived 3D Fe-N-S co-doped carbon matrix/nanotube nanocomposites with advanced oxygen reduction activity and stability in both acidic and alkaline media, Appl. Catal. B Environ. 250 (2019) 143–149.
[13] Z. Wang, H. Jin, T. Meng, K. Liao, W. Meng, J. Yang, D. He, Y. Xiong, S. Mu, Fe, Cu-coordinated ZIF-derived carbon framework for efficient oxygen reduction reaction and zinc-air batteries, Adv. Funct. Mater. 28 (2018), 1802596.
[14] X. Yan, K. Liu, T. Wang, Y. You, J. Liu, P. Wang, X. Pan, G. Wang, J. Luo, J. Zhu, Atomic interpretation of high activity on transition metal and nitrogen-doped carbon nanofibers for catalyzing oxygen reduction, J. Mater. Chem. A 5 (2017) 3336–3345.
[15] Y. Xiong, Y. Yang, F.J. Disalvo, H.D. Abruna, Metal-organic-framework-derived Co-Fe bimetallic oxygen reduction electrocatalysts for alkaline fuel cells, J. Am. Chem. Soc. 141 (2019) 10744–10750.
[16] Z. Ma, S. Li, L. Wu, L. Song, G. Jiang, Z. Liang, D. Su, Y. Zhu, R.R. Adzic, J.X. Wang, Z. Chen, NbOx nano-nail with a Pt head embedded in carbon as a highly active and durable oxygen reduction catalyst, Nano Energy 69 (2020), 104455.
[17] Z. Song, M. Norouzi, L. Zhang, B. Wang, L. Yang, D. Banham, Y. Zhao, J. Liang, M. Zheng, R. Li, S. Ye, X. Xun, Origin of achieving the enhanced activity and stability of Pt electrocatalysts with strong metal-support interactions via atomic layer deposition, Nano Energy 53 (2018) 716–725.
[18] Z. Yang, Y. Wang, M. Zhu, Z. Li, W. Chen, W. Wei, T. Yuan, Y. Qu, Q. Xu, C. Zhao, X. Wang, P. Li, Y. Li, Y. Wu, Y. Li, Boosting oxygen reduction catalysis with Fe-N_4 sites decorated porous carbons toward fuel cells, ACS Catal. 9 (2019) 2158–2163.
[19] H. Zhang, H.T. Chung, D.A. Cullen, S. Wagner, U.I. Kramm, K.L. More, P. Zelenay, G. Wu, High-performance fuel cell cathodes exclusively containing atomically dispersed iron active sites, Energy Environ. Sci. 12 (2019) 2548–2558.
[20] H. Jin, Z. Kou, W. Cai, H. Zhou, P. Ji, B. Liu, A. Radwan, D. He, S. Mu, P-Fe bond oxygen reduction catalysts toward high-efficiency metal-air batteries and fuel cells, J. Mater. Chem. A 8 (2020) 9121–9127.
[21] L. Zhang, K. Doyle-Davis, X. Sun, Pt-Based electrocatalysts with high atom utilization efficiency: from nanostructures to single atoms, Energy Environ. Sci. 12 (2019) 492–517.
[22] M. Shen, M. Xie, J. Slack, K. Waldrop, Z. Chen, Z. Lyu, S. Cao, M. Zhao, M. Chi, P. N. Pintauro, R. Cao, Y. Xia, Pt-Co truncated octahedral nanocrystals: a class of highly active and durable catalysts toward oxygen reduction, Nanoscale 12 (2020) 11718–11727.
[23] M. Xiao, J. Zhu, G. Li, N. Li, S. Li, Z.P. Cano, L. Ma, P. Cui, P. Xu, G. Jiang, H. Jin, S. Wang, T. Wu, J. Lu, A. Yu, D. Su, Z. Chen, Single-atom iridium heterogeneous catalyst in oxygen reduction reaction, Angew. Chem. Int. Ed. 58 (2019) 9640–9645.
[24] F. Kong, Z. Ren, M. Norouzi Banis, L. Du, X. Zhou, G. Chen, L. Zhang, J. Li, S. Wang, M. Li, K. Doyle-Davis, Y. Ma, R. Li, A. Young, L. Yang, M. Markiewicz, Y. Tong, G. Yin, C. Du, J. Luo, X. Sun, Active and stable Pt-Ni alloy octahedra catalyst for oxygen reduction via near-surface atomical engineering, ACS Catal. 10 (2020) 4205–4214.
[25] G. Zhang, M. Norouzi Banis, Q. Wei, M. Cai, Y. Zhang, R. Li, S. Sun, X. Sun, Pt/TiSix-NCNT novel janus nanostructure: a new type of high-performance electrocatalyst, ACS Appl. Mater. Interfaces 10 (2018) 10771–10777.
[26] Y. Xiong, Y. Yang, F.J. Disalvo, H.D. Abruña, Pt-decorated composition-tunable Pd-Fe@Pd/C core-shell nanoparticles with enhanced electrocatalytic activity toward the oxygen reduction reaction, J. Am. Chem. Soc. 140 (2018) 7248–7255.
[27] Q. Liu, L. Du, G. Fu, Z. Cui, Y. Li, D. Dang, X. Gao, Q. Zheng, J.B. Goodenough, Structurally ordered Fe_3Pt nanoparticles on robust nitride support as a high performance catalyst for the oxygen reduction reaction, Adv. Energy Mater. 9 (2019), 1803040.
[28] Y. Li, Q. Li, H. Wang, L. Zhang, D.P. Wilkinson, J. Zhang, Recent progresses in oxygen reduction reaction electrocatalysts for electrochemical energy applications, Electrochem. Energy Rev. 2 (2019) 518–538.
[29] D. He, H. Tang, Z. Kou, M. Pan, X. Sun, J. Zhang, S. Mu, Engineered graphene materials: synthesis and applications for polymer electrolyte membrane fuel cells, Adv. Mater. 29 (2017).
[30] Y. Bian, H. Wang, Z. Gao, J. Hu, D. Liu, L. Dai, A facile approach to high-performance trifunctional electrocatalysts by substrate-enhanced electroless deposition of Pt/NiO/Ni on carbon nanotubes, Nanoscale 12 (2020) 14615–14625.
[31] M. Zhang, Q. Dai, H. Zheng, M. Chen, L. Dai, Novel MOF-derived Co@N-C bifunctional catalysts for highly efficient Zn-air batteries and water splitting, Adv. Mater. 30 (2018), 1705431.
[32] X. Lu, B. Xia, S. Zang, X. Lou, Metal-organic frameworks based electrocatalysts for the oxygen reduction reaction, Angew. Chem. Int. Ed. 59 (2020) 4634–4650.
[33] X. Wang, D.A. Cullen, Y.T. Pan, S. Hwang, M. Wang, Z. Feng, J. Wang, M. H. Engelhard, H. Zhang, Y. He, Y. Shao, D. Su, K.L. More, J.S. Spendelow, G. Wu, Nitrogen-coordinated single cobalt atom catalysts for oxygen reduction in proton exchange membrane fuel cells, Adv. Mater. 30 (2018) 1–11.
[34] B.K. Kang, S.Y. Im, J. Lee, S.H. Kwag, S. Bin Kwon, S.N. Tiruneh, M.J. Kim, J. H. Kim, W.S. Yang, B. Lim, D.H. Yoon, In-situ formation of MOF derived mesoporous Co_3N/amorphous N-doped carbon nanocubes as an efficient electrocatalytic oxygen evolution reaction, Nano Res. 12 (2019) 1605–1611.
[35] X. Wan, X. Liu, Y. Li, R. Yu, L. Zheng, W. Yan, H. Wang, M. Xu, J. Shui, Fe-N-C electrocatalyst with dense active sites and efficient mass transport for high-performance proton exchange membrane fuel cells, Nat. Catal. 2 (2019) 259–268.
[36] X. Chen, L. Yu, S. Wang, D. Deng, X. Bao, Highly active and stable single iron site confined in graphene nanosheets for oxygen reduction reaction, Nano Energy 32 (2017) 353–358.
[37] H. Yang, X. Wang, Secondary-component incorporated hollow MOFs and derivatives for catalytic and energy-related applications, Adv. Mater. 31 (2019), 1800743.
[38] M. Xiao, H. Zhang, Y. Chen, J. Zhu, L. Gao, Z. Jin, J. Ge, Z. Jiang, S. Chen, C. Liu, W. Xing, Identification of binuclear Co_2N_5 active sites for oxygen reduction reaction with more than one magnitude higher activity than single atom CoN_4 site, Nano Energy 46 (2018) 396–403.
[39] C. Zhang, P. Wang, W. Li, Z. Zhang, J. Zhu, Z. Pu, Y. Zhao, S. Mu, MOF-Assisted synthesis of octahedral carbon-supported PtCu nanoalloy catalysts for an efficient hydrogen evolution reaction, J. Mater. Chem. A 8 (2020) 19348–19356.
[40] L. Chong, J. Wen, J. Kubal, F.G. Sen, J. Zou, J. Greeley, M. Chan, H. Barkholtz, W. Ding, D.J. Liu, Ultralow-loading platinum-cobalt fuel cell catalysts derived from imidazolate frameworks, Science 362 (2018) 1276–1281.
[41] L. Zhang, J.M.T.A. Fischer, Y. Jia, X. Yan, W. Xu, X. Wang, J. Chen, D. Yang, H. Liu, L. Zhuang, M. Hankel, D.J. Searles, K. Huang, S. Feng, C.L. Brown, X. Yao, Coordination of atomic Co-Pt coupling species at carbon defects as active sites for oxygen reduction reaction, J. Am. Chem. Soc. 140 (2018) 10757–10763.
[42] X. Ao, W. Zhang, B. Zhao, Y. Ding, G. Nam, L. Soule, A. Abdelhafiz, C. Wang, M. Liu, Atomically dispersed Fe-N-C decorated with Pt-alloy core–shell nanoparticles for improved activity and durability towards oxygen reduction, Energy Environ. Sci. 13 (2020) 3032–3040.
[43] D. He, L. Zhang, D. He, G. Zhou, Y. Lin, Z. Deng, X. Hong, Y. Wu, C. Chen, Y. Li, Amorphous nickel boride membrane on a platinum-nickel alloy surface for enhanced oxygen reduction reaction, Nat. Commun. 7 (2016) 12362.
[44] Y. Pan, K. Sun, S. Liu, X. Cao, K. Wu, W.C. Cheong, Z. Chen, Y. Wang, Y. Li, Y. Liu, D. Wang, Q. peng, C. Chen, Y. Li, Core-shell ZIF-8@ZIF-67 derived CoP nanoparticles-embedded N-doped carbon nanotube hollow polyhedron for efficient over-all water splitting, J. Am. Chem. Soc. 140 (2018) 2610–2618.
[45] H. Zhong, Y. Luo, S. He, P. Tang, D. Li, N. Alonso-Vante, Y. Feng, Electrocatalytic cobalt nanoparticles interacting with nitrogendoped carbon nanotube in situ generated from a metal-organic framework for the oxygen reduction reaction, ACS Appl. Mater. Interfaces 9 (2017) 2541–2549.
[46] H. Bin Yang, J. Miao, S.F. Hung, J. Chen, H.B. Tao, X. Wang, L. Zhang, R. Chen, J. Gao, H.M. Chen, L. Dai, B. Liu, Identification of catalytic sites for oxygen reduction and oxygen evolution in N-doped graphene materials: development of highly efficient metal-free bifunctional electrocatalyst, Sci. Adv. 2 (2016) 1–12.
[47] Y. Gao, T. Li, Y. Zhu, Z. Chen, J. Liang, Q. Zeng, L. Lyu, C. Hu, Highly nitrogen-doped porous carbon transformed from graphitic carbon nitride for efficient metal-free catalysis, J. Hazard. Mater. 393 (2020), 121280.
[48] Y. Ha, B. Fei, X. Yan, H. Xu, Z. Chen, L. Shi, M. Fu, W. Xu, R. Wu, Atomically dispersed Co-pyridinic N-C for superior oxygen reduction reaction, Adv. Energy Mater. 10 (2020), 2002592.
[49] J. Xu, C. Zhang, H. Liu, J. Sun, R. Xie, Y. Qiu, F. Lü, Y. Liu, L. Zhuo, X. Liu, J. Luo, Amorphous MoO_X-stabilized single platinum atoms with ultrahigh mass activity for acidic hydrogen evolution, Nano Energy 70 (2020), 104529.
[50] M.S. Faber, S. Jin, Earth-abundant inorganic electrocatalysts and their nanostructures for e nergy conversion applications, Energy Environ. Sci. 7 (2014) 3519–3542.

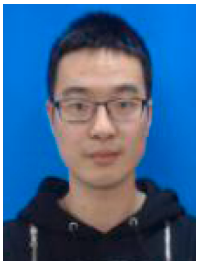

Lvhan Liang received his B.E. degree in 2017 from polymer materials and engineering of Hubei University. Currently he is a research master of State Key Laboratory of Advanced Technology for Materials Synthesis and Processing, Wuhan University of Technology. His current research topic is the construction of heterostructures of supported metal single-atom clusters and the study of electrocatalytic performance.

Huihui Jin received her BE, MSc and PhD degree in 2013, 2015 and 2020 from Wuhan University of technology. Now she is a postdoctor in Wuhan University of technology. Her current research interests lie in the development of non-precious metal for electrocatalysis and electrochemical sensor.

Huang Zhou obtained his M.S. in Materials Science and Engineering under the supervision of Prof. Shichun Mu in 2017 from Wuhan University of Technology. In 2020, he obtained his PhD degree under supervision of Prof. Yuen Wu and Yadong Li at iChEM (Collaborative Innovation Centre of Chemistry for Energy Materials), University of Science and Technology of China. Now, he is a Postdoctoral Fellow at iChEM. His research interests focus on the design and construction of nano or sub-nano catalysts in energy conversion and storage.

Bingshuai Liu received respectively his BE and BEc degree from the School of Materials Science and Engineering and Business School at University of Jinan in 2018. He is currently a research master in school of Material Science and Engineering from Wuhan University of Technology. His research interests focus on metal-organic frameworks (MOFs) and their applications in electrochemical energy storage.

Chenxi Hu received her BE degree from Henan University of Science and Technology in 2017. Now she is a master student in fuel cell at Wuhan University of Technology. Her research interests focus on metal-organic frameworks (MOFs) and the development of non-precious metal for electrocatalysis.

Ding Chen received his B.E. degree in 2018 from Huainan Normal University in Material Chemistry. Currently he is a research master of State Key Laboratory of Advanced Technology for Materials Synthesis and Processing, Wuhan University of Technology. Now his research topic is the application of transition metal phosphates in hydrogen production by electrolysis of water.

Zhe Wang is a Ph.D. candidate at School of Science, Wuhan University of Technology (WUT). He received his B.S. and M.S. degree at School of Chemical and Biological Engineering in Changsha University of Science & Technology (2015) and State Key Laboratory of Advanced Technology for Materials Synthesis and Processing in WUT (2018), respectively. His research is mainly focused on graphene-based film materials for electromagnetic interference shielding, strain sensors and mechanics.

Zhiyi Hu is an associate professor within the NRC (Nanostructure Research Centre) at Wuhan University of Technology. He received his PhD degree in Physics from the University of Antwerp in 2016. His research focuses on nanostructured materials and interface characterization using advanced electron microscopy, including HR-(S)TEM, STEM-EELS and 3D electron tomography

Yufeng Zhao is currently working as a professor at Shanghai University. She received her B.S. and M.S. degree from Tianjin University, China. She obtained her Ph.D. from Nanyang Technological University, Singapore. Afterwards, she worked in Deakin University, Australia (2006–2008) and Phillips University Marburg, Germany (2008–2009) as a research scientist. She was also a visiting professor in Northwestern University (2014–2015). Her research mainly focuses on energy storage materials and devices, such as nanocarbon materials, sodium ion batteries, and electrocatalysts.

Hai-Wen Li is a Professor at Hefei General Machinery Research Institute. From 2005 to 2011, he worked as Postdoc, JSPS Postdoctoral Fellow and Assistant Professor at Institute for Materials Research, Tohoku University. From 2011 to 2020, he served as an Associate Professor at International Research Center for Hydrogen Energy and International Institute for Carbon-Neutral Energy Research, Kyushu University. His research activities mainly focus on the development of advanced materials and systems for hydrogen storage and energy storage.

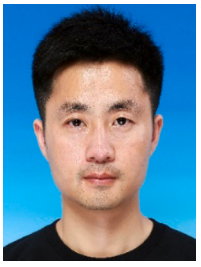

Daping He is a full professor at Wuhan University of Technology. He obtained his Ph.D. degree in Materials Processing Engineering from Wuhan University of Technology in 2013. He was a Postdoctoral Fellow in the University of Science and Technology of China. Then he joined University of Bath as a Newton International Fellow and University of Cambridge as a Postdoctoral Fellow. His research interest is preparation and application of nano composite materials into new energy devices, sensors and RF microwaves field. He has published over 80 peer-reviewed papers and 20 Chinese patents.

Dr. Shichun Mu is Chair Professor at Wuhan University of Technology. He received his Ph.D. degree from Chinese Academy of Sciences, China in 2001. Afterwards, he joined the Wuhan University of Technology as a postdoctoral researcher in 2001–2003. Since 2006, he has been a full professor at Wuhan University of Technology. He was an academic visitor at Inorganic Chemistry Laboratory, University of Oxford in 2007–2008. His research focuses on nanocarbon materials, PEM fuel cell/water splitting electrocatalysts, and metal-air batteries, lithium-ion batteries related materials and devices. He has published over 200 peer reviewed papers.